SYNTHETIC RUBIES BY DOUROS: A NEW CHALLENGE FOR GEMOLOGISTS

By Henry A. Hänni, Karl Schmetzer, and Heinz-Jürgen Bernhardt

Greek manufacturer J. & A. Douros introduced a new flux synthetic ruby in early 1993. Grown by spontaneous nucleation in a lead-based solvent, the Douros synthetic ruby occurs as rhombohedral single crystals and twinned tabular crystals, as well as in clusters. The tabular crystals typically have intense red cores that gradually decrease in saturation to a near-colorless outermost layer; the rhombohedral crystals have a deep red body and a thin near-colorless layer on the rhombohedral faces, with umbrella-like growth patterns in some areas. Some samples contain distinctive inclusions of yellow residual flux with spherical bubbles. Chemically, the crystals are heavily zoned, and EDXRF analyses revealed variable trace amounts of Ti, Fe, Cr, and Ga, as well as some Pb. SEM-EDS identified the flux particles as lead bearing. Microprobe analyses showed high Cr values in the crystal cores; in certain growth zones, Fe replaces Cr in the outermost layers. If inclusions or typical growth structures are not present, chemical composition appears to be the best means of separating these Douros synthetic rubies from natural rubies.

ABOUT THE AUTHORS

Dr. Hänni is director of SSEF Swiss Gemological Institute, Zurich, and associate professor of gemology at Basel University, Switzerland. Dr. Schmetzer is a research scientist residing in Petershausen near Munich, Germany. Dr. Bernhardt is a research scientist at the Institute for Mineralogy of Ruhr-University, Bochum, Germany.

Acknowledgements appear at end of article.

Gems & Gemology, *Vol. 30, No. 2, pp. 72–86.*

Recently, a new type of flux-grown synthetic ruby entered the gem market (figure 1). Manufactured by J. & A. Douros Created Gems in Piraeus, Greece, the Douros synthetic ruby poses new challenges for gemologists. Like the Ramaura flux-grown synthetic rubies introduced in 1982 (Bosshart, 1983; Kane, 1983), stones faceted from the Douros laboratory-grown crystals may create considerable difficulties for identification. Standard gemological tests are inadequate for clean or only slightly included samples. Even with advanced tests such as U.V.–visible spectrophotometry, EDXRF chemical analysis, or identification of growth planes, the present material may cause difficulties in identification (see, e.g., Hänni and Bosshart, 1993; Hänni and Schmetzer, 1993; and Smith and Bosshart, 1993).

This article reports on our examination of several crystals and faceted samples of the Douros material. To help establish criteria by which the Douros synthetic rubies can be separated from their natural counterparts, we will describe in detail the mineralogical, gemological, and chemical characteristics of this new flux-grown synthetic ruby.

PRODUCTION

Brothers John and Angelos Douros run a small family business that manufactures synthetic crystals. A physicist and an electrical engineer, respectively, they previously specialized in refining precious metals. With furnaces they built themselves, the Douros brothers use controlled spontaneous nucleation and slow cooling techniques to produce synthetic rubies by unseeded flux growth (J. Douros, pers. comm., 1993).

After some years of experimentation, in January 1993 they presented the material to the public for the first time, at the Athens Jewellery Fair. Simultaneously, they reported on their new synthetic ruby in the Greek jewelry magazine *Chrysotechni* (Douros and Douros, 1993).

At present, the Douros brothers use two furnaces in

Figure 1. This 44.74-ct rhombohedral crystal and the accompanying cut stones (from left to right—4.93, 2.55, 2.14, and 3.51 ct) are representative of some of the Douros flux-grown synthetic rubies that have been produced to date. Samples courtesy of John Douros, Piraeus, Greece; photo by Robert Weldon.

which exact temperature control permits very slow cooling and, thus, steady crystal growth that incorporates the chemical constituents needed to duplicate natural ruby as closely as possible (J. Douros, pers. comm., 1993). They dope the flux with various trace elements in their effort to reproduce the different shades of color and trace-element compositions encountered among natural rubies. As is typically the case with flux-grown synthetics, the production costs are significantly higher than for synthetic ruby crystals produced by the Verneuil or Czochralski methods. The Douros flux method typically yields crystals up to 20 to 50 ct; the largest crystal produced to date is 70 grams (350 ct) and the largest faceted stone, 8.5 ct. In June 1994, John Douros reported that they were producing approximately 2,000 ct per month, but expected this quantity to increase. The precise conditions of growth and composition of the flux are proprietary and were not revealed to the authors. The material is being sold through various channels.

MATERIALS AND METHODS

For this study, we obtained 12 synthetic ruby crystals (2–17 ct) and 10 faceted synthetic rubies (1–5 ct) directly from the Douros brothers. To best examine the inclusions, we polished one or two faces on some of the crystals.

For gemological testing, we used a Topcon refractometer with a sodium light source, a Mettler balance with specific-gravity attachment, a Zeiss Jena 7° dispersion spectroscope with Eickhorst base, a standard ultraviolet lamp (long-wave and short-wave) with dark box, a Schneider immersion microscope with Zeiss optics, and a Wild Stereozoom microscope with Eickhorst Multiscope base. We used methylene iodide as the immersion liquid (with a special sample holder) for examination and photomicrography of the samples.

Polarized absorption spectra for the e- and o-vibrations were recorded on two crystals, one crystal slice, and one faceted sample. We used Hitachi 4001 and Pye-Unicam SP8-100 spectrophotometers with polarization filters, the crystals oriented with the c-axis perpendicular to the incident beam (see, e.g., Bosshart, 1982). Qualitative chemical investigations, by energy-dispersive X-ray fluorescence analysis (EDXRF; see, e.g., Stern and Hänni, 1982; Muhlmeister and Devouard, 1991), were performed on 13 samples (as well as, subsequently, on sections cut and polished from two of these samples) using a Philips PV 9500 X-ray generator and detectors with a Spectrace TX-6100 system and software package. Quantitative chemical analyses were performed on seven of the same samples with a CAMECA Camebax SX 50 electron microprobe. The electron microprobe analyses (EPMA) included 30 point analyses on table facets of three faceted synthetic rubies and on a rhombohedral face of one rhombohedral crystal, as well as 30 point analyses on the

Figure 2. The 10.37-ct tabular crystal (inset), two rhombohedral crystals (44.74 and 13.69 ct), and 167.97-ct crystal cluster shown here represent the Douros crystals observed thus far. Photo by Robert Weldon. Inset photo by Maha DeMaggio.

two new surfaces produced when an irregular intergrowth of two rhombohedral crystals (samples D1 and D2) of random mutual orientation was sawn and polished. For the microscopic examination of one of the tabular crystals (to obtain a cross-section between the two basal pinacoids), we had a slice cut perpendicular to the basal pinacoid *c*. Three microprobe scans of 50 point analyses each were performed on this 2.2-mm-thick polished slab on the surface at the cross-section.

A Philips scanning electron microscope (SEM 515) with a Tracor energy-dispersive X-ray spectrometer (EDS) system was used to investigate the surfaces of one rough and one cut Douros synthetic ruby in order to identify the chemical components of yellow material and metallic particles on those surfaces. We also submitted some of the yellow material removed from the surface of one of the crystals to X-ray powder diffraction analysis with a Gandolfi camera.

Figure 3. As is evident in this schematic drawing of a rhombohedral crystal of Douros synthetic ruby, three crystal faces are well developed: the dominant basal plane c *(0001), the positive rhombohedron* r *(10$\bar{1}$1), and the subordinate negative rhombohedron* d *(01$\bar{1}$2).*

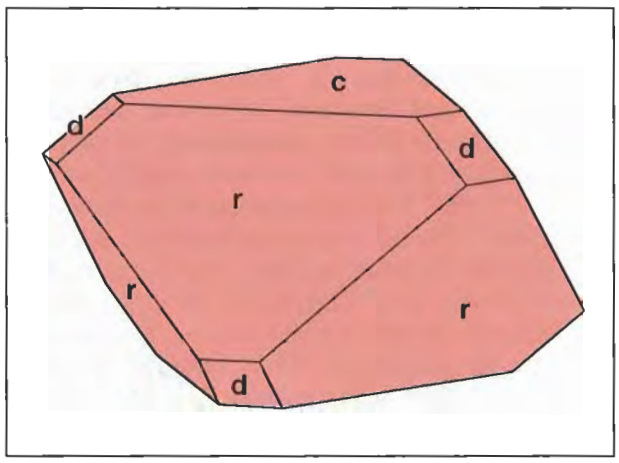

CRYSTALLOGRAPHY

The Douros flux-grown synthetic ruby crystals occur in two habits: rhombohedral (see, e.g., figures 1–3) and tabular (figures 2 and 4). There are also crystals intermediate between these two basic types as well as intergrown clusters (figure 2). In all the samples we examined, we noted that only three crystal faces are developed: the basal pinacoid *c* (0001), the positive rhombohedron *r* (10$\bar{1}$1), and the negative rhombohedron *d* (01$\bar{1}$2). Trigonal growth structures were typically seen on rhombohedral and tabular crystals alike (again, see figure 2).

As illustrated in figure 3, the rubies with tabular habit have a dominant basal plane *c*; the rhombohedral faces *r* and *d* are small. Occasionally, they also show small, colorless "satellite" corundum crystals that have intergrown with the main crystal; rarely, metallic flakes of platinum (from the crucible; figure 5) or a yellow material (figure 6) are found on the surface.

Most of the tabular crystals are penetration twins, with the two components symmetrically related by a 180° rotation about the c-axis. This twinning is identical to a reflection across one of

the first-order hexagonal prism faces $\{10\bar{1}0\}$ or across the basal pinacoid {0001}. The two components of the twinned individuals are in contact along four twin boundaries, which are oriented parallel to the twin planes $\{10\bar{1}0\}$ and {0001}, respectively (figure 4; see, e.g., Schmetzer et al., 1994).

The rhombohedral crystals are more equidimensional and thus better suited for cutting. They are basically formed by dominant basal and rhombohedral faces, *c* and *r*, with somewhat smaller *d* faces (again, see figure 3). We did not see prism faces on any of our samples, but we did see small hexagonal dipyramids *n* $\{22\bar{4}3\}$ on one crystal. We did not observe twinning in any of the rhombohedral crystals.

These two habits of Douros synthetic rubies are similar to those described for Ramaura flux-grown synthetic rubies (Kane, 1983; Schmetzer, 1986a and b). The penetration twinning seen in the Douros synthetic rubies is identical to that commonly seen in Ramaura synthetic rubies (as described in Schmetzer et al., 1994), but different from twinning in other flux-grown synthetic rubies, such as those produced by Chatham Created Gems. However, whereas we observed twinning only in tabular Douros crystals, most twinned Ramaura synthetic ruby crystals observed up to now are of rhombohedral habit.

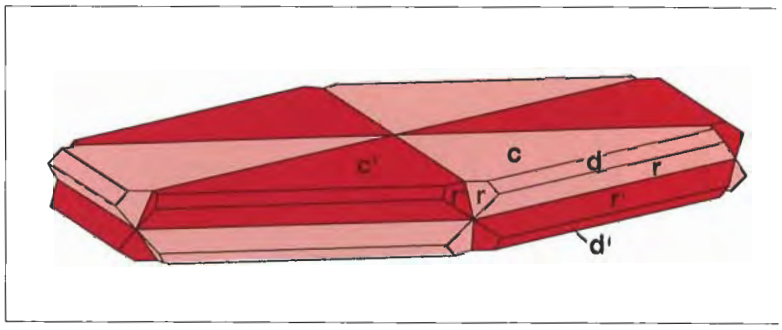

Figure 4. This schematic drawing of a tabular Douros synthetic ruby crystal shows the dominant c *planes and the subordinate* r *and* d *faces. The sample illustrated is actually a penetration twin, which is frequently encountered in this material. The second crystal is denoted by the darker color and its relative faces marked* c', r', *and* d'.

COLOR AND COLOR ZONING

The samples ranged from saturated red to purplish red and reddish purple (see, e.g., figures 1 and 2), depending on the amounts of chromium, titanium, and iron present in each. The different concentrations of color-causing trace elements also produced geometrically bounded color zoning within the crystals. In the tabular crystals only, we noted: (1) near-colorless to light red outermost zones confined to *r* and *d* faces (figure 7); (2) near-colorless to light red triangular growth sectors confined to twin boundaries (figure 8); and (3) purple to bluish purple color bands running parallel to both rhombohedral faces *r* and *d* (figure 9). In both the rhombohedral and tabu-

Figure 5. A small satellite crystal and a shiny grain of platinum (from the crucible) can be seen on the surface (basal face c*) of this tabular crystal. The crazed orange area is enclosed flux that lies below the surface. Magnified 50×.*

Figure 6. On the surfaces of some of the crystals, we saw pits filled with a yellow polycrystalline material. Magnified 6×.

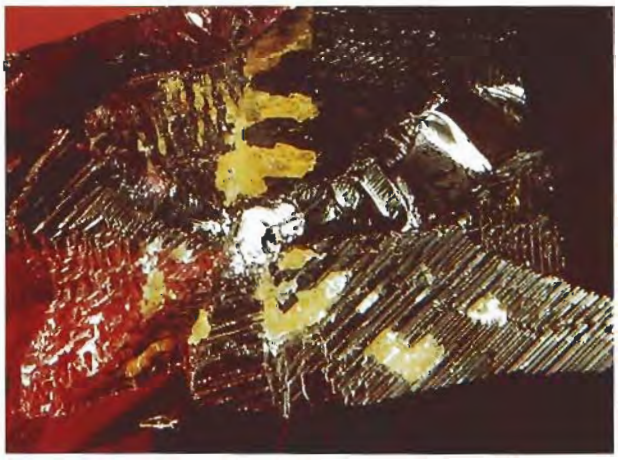

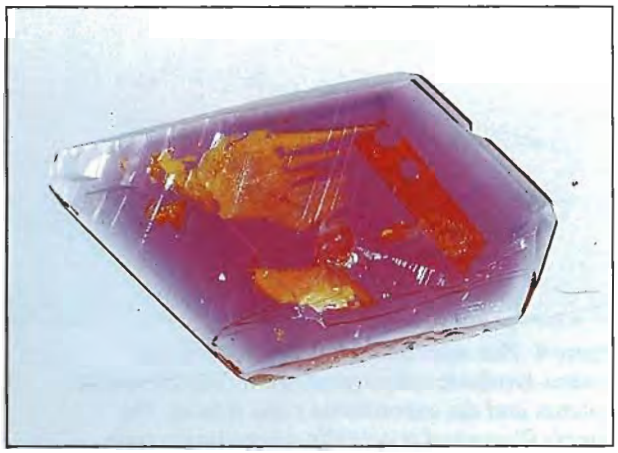

Figure 7. This 34-mm-diameter tabular Douros synthetic ruby crystal exhibits the near-colorless outermost zone typical of this form. Note also the large pieces of yellow flux that have been trapped in the crystal. The flux is typically oriented parallel to the basal face.

Figure 8. On the edge of a tabular crystal, a near-colorless to light red triangular growth sector is confined to twin boundaries. Immersion, magnified 25×.

lar crystals, we saw purple to bluish purple intercalated acute-angle triangles (figures 9 and 10). The purple to bluish purple bands and triangular zones represent a distinct blue-sapphire component within the synthetic ruby (cf. Schmetzer and Bank, 1981).

GEMOLOGICAL PROPERTIES

Table 1 gives the gemological properties for the 10 faceted Douros synthetic rubies and 12 crystals (eight rhombohedral and four tabular). Because R.I. and density readings overlap those of natural rubies, they are not useful in identifying this material as synthetic. Note, however, that the R.I.'s measured on the rhombohedral faces of rhombohedral crystals are somewhat lower than the values obtained from the basal pinacoids. The latter correspond to the R.I.'s of the faceted samples. The basal-pinacoid R.I.'s of the tabular crystals were similar to those from rhombohedral faces of the rhombohedral crystals. On a plane cut perpendicular through the basal pinacoids of a tabular crystal, no distinct readings could be obtained. These differences in R.I. are undoubtedly related to differences in chemical composition—especially the differential incorporation of chromium (which tends to increase R.I.)—between the body of the crystal and its outermost layers.

Figure 9. Purple to bluish purple color bands (like the one shown here in the lower part of the photo) were occasionally seen in tabular Douros synthetic ruby crystals, as were acute-angle purple to bluish purple triangular growth zones (like the one seen here in the lower left). A distinct iron/titanium component, in addition to the chromium component of ruby, is responsible for this color zoning. The inclusions shown here are flux. Magnified 10×.

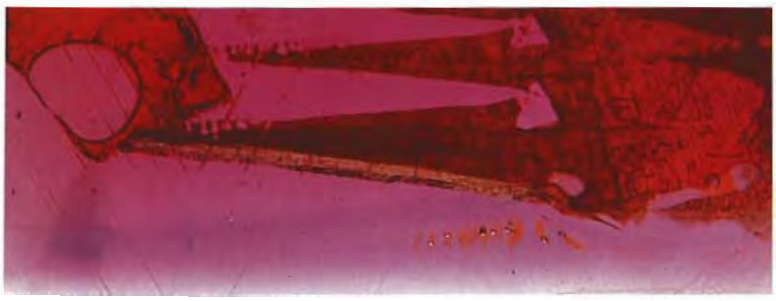

The strong red fluorescence to ultraviolet radiation (more pronounced to long-wave) of the faceted Douros synthetic rubies is characteristic for low iron-bearing rubies, so it cannot be used to identify the synthetic material. The absence of fluorescence in some of the outermost areas of the Douros crystals appears to be due to the selective chemistry on the faces (see below) and, again, to the lower chromium content in the outermost layers. The resulting appearance of the crystals has been described as a layer of yellowish orange fluorescence on some of the outside faces to long-wave U.V. radiation, or a moderate to strong whitish blue fluorescence to short-wave U.V. Because these inert to pale-colored

portions of the crystals are generally removed during cutting, the fluorescence of the faceted Douros synthetic rubies is typically a uniform red.

MICROSCOPIC CHARACTERISTICS

Structural Properties (Growth Features and Twinning). The internal growth features of both the rough and the faceted Douros samples correspond to the external morphology of the crystals. We identified internal growth planes parallel to all three macroscopically observed crystal faces *c*, *r*, and *d*. Although similar growth planes are also found in Ramaura and Chatham flux-grown synthetic rubies (Schmetzer, 1987), there are three types of growth patterns that appear to be most characteristic of rhombohedral Douros synthetic rubies (table 2).

In most of the rhombohedral crystals, we recognized a growth pattern that is evident as areas of different colors with sharply defined boundaries. The main body color between the basal planes is intense red, whereas the thin outermost layers confined to the *r* and *d* faces are near-colorless to light red (figure 11). These outer layers represent the latest growth stage.

All of the rhombohedral crystals showed faces parallel to the negative rhombohedron *d*. Such faces were prominent (although smaller than *c* and *r*) on the actual surface of the crystals, which represents the latest growth period. In earlier stages of growth (i.e., more toward the center of the crystal) the *d* faces were smaller. In the earliest growth stage, in the center of the crystal, growth parallel to *d* was absent, and the surface of the crystal at that stage was defined just by *r* and *c* faces. When a rhombohedral Douros synthetic ruby crystal was viewed with immersion in the microscope, in most cases the area confined to *d* growth showed a distinct, curved, umbrella-like outline, because this part of the crystal has a higher saturation of red compared to neighboring zones (figure 12). In some cases, the

Figure 10. Acute-angle color zoning was also seen in rhombohedral Douros synthetic ruby crystals. Compare the appearance of the zone in this sample with that in the tabular Douros crystal in figure 9. Again, the bluish purple color is due to (Fe,Ti)-rich zones within the ruby crystal. Immersion, magnified 40×.

TABLE 1. Gemological properties of Douros synthetic rubies.[a]

Property	Rhombohedral crystals	Faceted samples	Tabular crystals
Density (g/cm³)	3.993 – 4.010	3.997 – 4.015	4.023 – 4.029
Refractive indices	Basal pinacoid *c*: n_o 1.771 – 1.773 n_e 1.763 – 1.765 Pos. rhombohedron *r*: n_o 1.768 – 1.770 n_e 1.760 – 1.762	n_o 1.772 – 1.774 n_e 1.762 – 1.764	Basal pinacoid *c*: n_o 1.768 – 1.771 n_e 1.760 – 1.763 Plane cut and polished perpendicular to *c*: no distinct reading
Pleochroism			
∥*c*	Yellowish red to red	Yellowish red to red	Yellowish red to red
⊥*c*	Purplish red	Purplish red	Purplish red
Fluorescence			
LWUV	Intense orangy red, inert in the surface layer confined to *r* and *d*	Intense red	Intense orangy red, inert in the surface layer confined to *c*, *r*, and *d*
SWUV	Moderate red, inert in the surface layer confined to *r* and *d*	Moderate red	Moderate red, inert in the surface layer confined to *c*, *r*, and *d*

[a]*As recorded for eight rhombohedral crystals, 10 faceted samples, and four tabular crystals.*

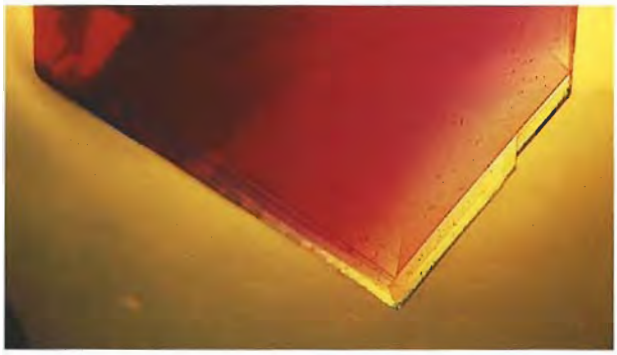

Figure 11. The thin outermost layers confined to the r *and* d *faces that form the sharp edge of this rhombohedral crystal are near-colorless to light red. Note that there is no colorless layer on the basal faces (here, upper right and upper left). Immersion, magnified 25×.*

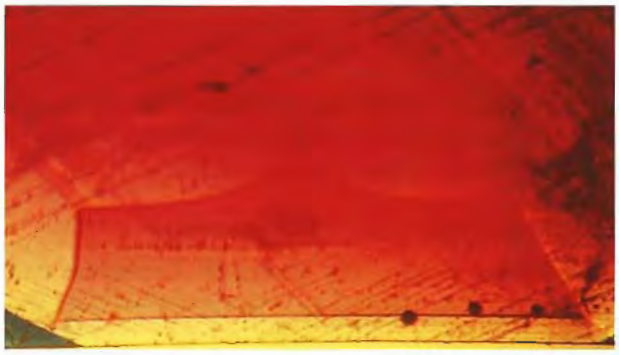

Figure 12. The growth sector formed by d*-face growth (at the bottom of the picture) in this rhombohedral crystal is defined by a distinctive umbrella-like boundary toward the neighboring* r *and* r' *face growth areas. Immersion, magnified 40×.*

d-face growth zones were confined to the outer areas of the crystal; the intermediate and central areas showed only growth parallel to *c* and *r* faces (figure 13).

Also in the rhombohedral crystals, as noted earlier, we occasionally saw acute-angle purple to bluish purple triangles that lie in the red core (again, see figure 10). These areas undoubtedly contain a distinct blue sapphire (Fe, Ti) component in addition to the Cr content responsible for the ruby coloration.

In the tabular crystals, growth patterns includ-

TABLE 2. Crystallography, structural properties, and color zoning in Douros synthetic ruby crystals.[a]

Property	Rhombohedral crystals	Tabular crystals
Faces		
Basal pinacoid *c* (0001)	Dominant	Dominant
Pos. rhombohedron *r* ($10\bar{1}1$)	Dominant	Subordinate
Neg. rhombohedron *d* ($01\bar{1}2$)	Subordinate	Subordinate
Hexagonal dipyramid ($22\bar{4}3$)	Extremely small (in one sample)	Not observed
Twinning	Not observed	Penetration twinning
Growth patterns, color, color zoning		
c faces	Growth patterns present from the center to the surface; red; no color zoning, no boundary	Growth patterns present from the center to the surface; red in the center, continuous decrease in saturation toward the surface, and almost colorless in the outermost layer
r faces	Growth patterns present from the center to the surface; red; no color zoning from the center to a distinct boundary near the surface, with the outermost zone almost colorless	Growth patterns present from the center to the surface; red in the center, continuous decrease in saturation toward the surface, and almost colorless in the outermost zone
d faces	Growth patterns not present in the center, but begin to develop toward the surface; darker red (umbrella-type) growth structure; no color zoning from the beginning to a distinct boundary near the surface, with the outermost zone almost colorless	Growth patterns present from the center to the surface; dark red in the center, with a continuous decrease in saturation toward the surface; almost colorless in the outermost zone
Undetermined faces	Intercalated acute-angle purple to bluish purple triangles present	Intercalated acute-angle purple to bluish purple triangles present

[a]*As observed in eight rhombohedral and four tabular crystals examined.*

ed both regular and irregular distributions of color (again, see table 2). As a rule, there was no color zoning in the cores, and the outermost areas tended to be light red or near-colorless (again, see figure 7). The slice cut parallel to the c-axis of a twinned tabular crystal (on which microprobe analysis was also done) exhibits a rather complex growth pattern (figure 14). From the upper to the lower surface (i.e., from the *c* to the *-c* face), growth zones parallel to *c*, *r*, *d*, and *-c* can be seen. Both of the growth zones parallel to *c* and *-c* are colorless or light red on the surface. The color saturation increases toward the center of the crystal, which is saturated red. Growth areas confined to faces *r* and *d* are intense red in the center of the crystal, but they decrease in saturation in a direction parallel to the length of the slab, that is, toward the surfaces formed by the *r* and *d* faces. The outer zones of these areas are light red, merging to near-colorless next to the surface of the crystal. In the slice examined, the *d* growth zones are a more intense red than the adjacent *r* zones. This feature was also found in the rhombohedral crystals examined.

Purple-to bluish purple acute-angle zones were also observed in some of the tabular crystals; bands of similar color were seen in planes parallel to the rhombohedral faces (again, see figure 9). These represent areas rich in Fe and Ti.

Growth patterns of penetration twins on tabular crystals may be extremely complex in areas confined to one of the four boundaries of the synthetic ruby. In general, the differences are so subtle that these patterns are not useful to discriminate between natural and synthetic rubies. Therefore, synthetic stones faceted from these areas cannot be separated from natural ruby on the basis of growth structures alone.

We did not see colorless outer zones in any faceted samples, which indicates that this characteristic growth feature is removed during cutting. In two or three faceted samples, we saw part of the umbrella-type growth pattern, which indicates that they had been cut from crystals with rhombohedral habit. In one case, we found an irregularly outlined *d* growth zone in a "distorted" umbrella pattern (figure 15). Note that these zones become smaller toward the interior of the crystal. Therefore, it is possible that some Douros synthetic rubies cut from the cores of rhombohedral crystals might also lack any distinctive structural patterns. See Schmetzer (1986a

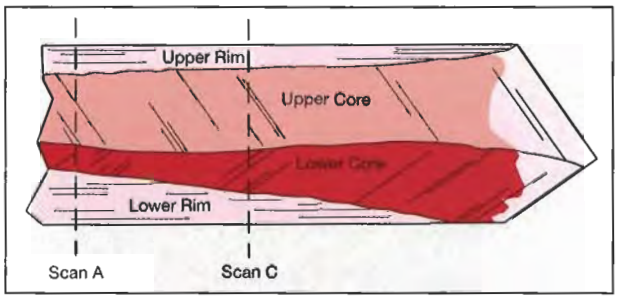

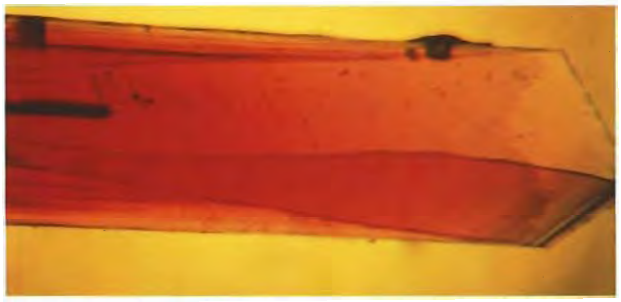

Figure 14. As illustrated in the line drawing, this slice from a tabular crystal cut parallel to the c-axis shows the large c *(upper) and* -c *(lower) faces, as well as the* r *and* d *faces that form the edge of the crystal. Internal growth zoning is accentuated here due to differences in trace-element chemistry. The darkest red zone is confined to the* d*-growth area. Immersion, magnified 25×. The positions of the two paths of microprobe point analyses (A and C) are shown in the schematic drawing. (Path B was located between paths A and C.)*

Figure 13. This rhombohedral Douros synthetic ruby crystal also revealed an umbrella-like growth sector confined to d *(intense red) as well as* r *and* r' *(light red), but the central part of the crystal shows only* r *and* r' *growth. Immersion, crossed polarizers; magnified 50×.*

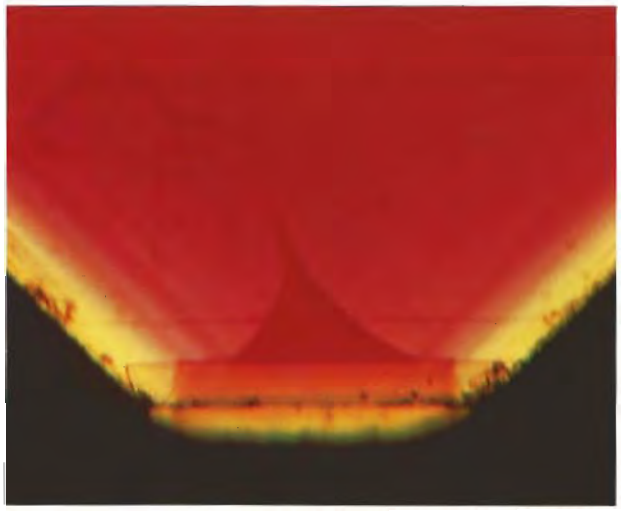

Figure 15. Structural characteristics are not always easy to recognize. Note this "distorted" umbrella pattern found in a faceted Douros synthetic ruby. These peculiar growth structures, with r, d, *and* r' *sectors, were observed in immersion at 50× magnification.*

and b) and Kiefert and Schmetzer (1991) for more on the method to identify growth planes.

Inclusions. Although many of the faceted samples appeared to be free of distinctive inclusions even at 40× magnification, some showed evidence of residual flux similar to that seen in other flux-grown synthetic rubies. Such inclusions may occur as larger, individual pieces of flux or as "veils" formed by many tiny droplets of flux. The former actually consist of coarse, rounded to elongated cavities that have been filled with a typically yellow substance and contain one or more voids or bubbles. Note that, in small amounts, the flux appears near-colorless; when present in larger volumes, the flux not only looks yellow but also reveals a distinctive crazed appearance and forms a mosaic-like pattern (figure 16). Occasionally, the flux inclusions are oriented parallel to the basal pinacoids, especially in twinned tabular crystals. In rhombohedral crystals, we have seen flat flux-containing inclusions oriented parallel to the rhombohedral faces.

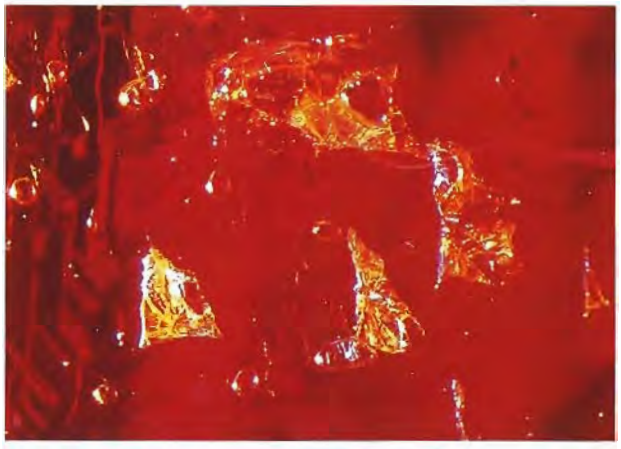

Figure 16. These pieces of yellow flux seen near the surface of a Douros synthetic ruby crystal are actually crazed residual fillings. Note the mosaic-like pattern of the flux, as well as the rounded voids or bubbles. Magnified 25×.

We saw rounded bubbles in nearly all of these flux inclusions (figure 17). Burch (1984) described similar two-phase inclusions for Kashan synthetic rubies. Most coarse flux is, as a rule, encountered near the surface of the crystals; that is, it was enclosed during the latest growth period.

The veil type of flux inclusion seen in the Douros synthetic rubies we examined (figure 18) looks very similar to patterns seen in heat- (and "borax-") treated natural ruby, which now represent most of the natural rubies encountered in the trade. Some of the flux particles are transparent, usually containing a bubble (figure 19).

Figure 17. This large piece of flux in a Douros synthetic ruby has a distinctive mosaic pattern and contains two bubbles. The fine lines—or "crazing"—in the solid part of the inclusion help distinguish such inclusions from two-phase inclusions that might be seen in a natural ruby. Immersion, magnified 25×.

For the most part, the Douros faceted synthetic rubies we examined were very clean, only slightly included, or the inclusions present resembled those seen in natural rubies (figure 20). They did not have platinum platelets or blades.

Optical Spectroscopy. The absorption spectra we observed with gemological desk-model spectroscopes do not differ from those of natural or synthetic rubies that have no (or little) iron content. That is, the Douros synthetic rubies show the well-known absorption lines in the red and blue regions of the spectrum, as well as the typical red fluorescence lines due to chromium.

The spectrophotometer results in the ultraviolet-visible range are also characteristic for rubies with Cr-only spectra (figure 21). Absorption minima for a typical sample lie at 328 and 471 nm for the o-vibration and at 328 and 481 nm for the e-vibration. Absorption maxima (i.e., broad bands) are centered at 410 and 560 nm for the o-vibration and 400 and 545 nm for the e-vibration. General absorption in the ultraviolet region is at 290 (e) and 280 nm (o), respectively. There were no significant differences in spectra among the various crystals or faceted samples.

When we calculated the spectral characteristics as proposed by Bosshart (1982), we determined typical values of λ_o and λ/W as 328/6.5 for the o-vibration and 326/5.8 for the e-vibration. These values overlap those for both Knischka synthetic rubies and natural rubies from Mogok. The minor spread of the plotting points within the Douros material is probably due to the trace-element variations encountered among different samples. Therefore, for the material examined so far, this method will not provide adequate distinction from natural rubies.

Figure 18. This veil-like inclusion in a faceted Douros synthetic ruby looks very similar to the networks of interconnecting channels seen in heat- (and "borax-") treated natural rubies. Magnified 50×.

Figure 19. These small flux inclusions, in parallel alignment, are transparent. Note that each contains a prominent bubble, which appears in high relief against the flux. The flux itself shows low relief against the ruby, which indicates that its refractive index is close to that of the ruby. Magnified 50×.

Chemistry. The EDXRF spectra showed the presence of chromium, titanium, and iron in varying

Figure 20. The presence of a fissure composed of tiny droplets, like that seen in this faceted Douros synthetic ruby, is of no help to a gemologist working only with a microscope. Such a pattern could also be seen in a natural ruby. Magnified 50×.

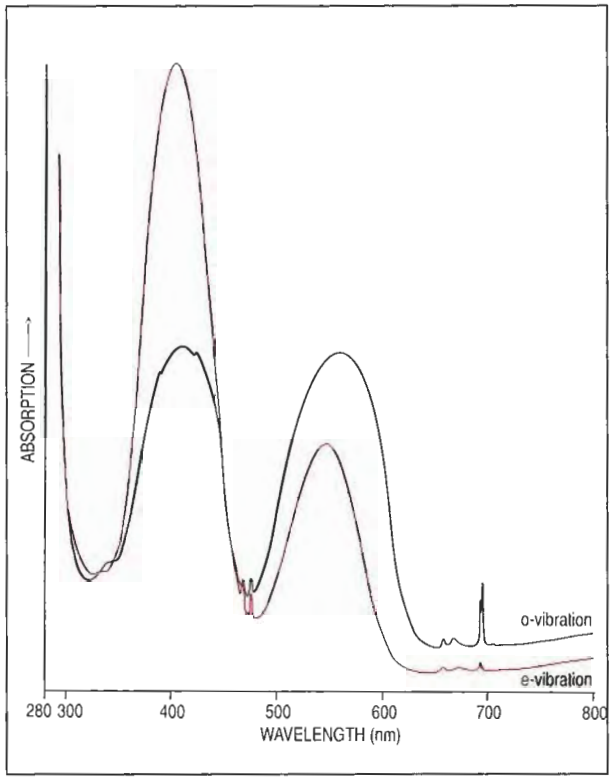

Figure 21. The U.V.–visible absorption spectra of the Douros synthetic rubies are similar to those of some natural rubies. These representative absorption spectra were taken with a Pye-Unicam SP8-100 spectrophotometer with polarization filter on a slice cut from a tabular Douros crystal. The sample was oriented with the c-axis perpendicular to the incident beam.

amounts (figure 22). In some cases, chromium peaks were dominant and only small amounts of iron were found. In other samples, distinct concentrations of both iron and chromium were observed. We noted the following variability in the peak heights for the prominent color-causing trace elements, iron and chromium (the letters in parentheses are keyed to the individual spectra in figure 22):

Fe > Cr on *c* faces of tabular crystals (A)

Fe > Cr on *r* faces of rhombohedral crystals (B)

Fe < Cr on *c* faces of rhombohedral crystals (C)

Fe < Cr on faceted stones (similar to C)

Titanium concentrations were always low, if present at all, and vanadium was at or below the detection limit of the instrument. Gallium signals were usually prominent.

The variability in, or absence of, certain color-causing elements (Ti, V, Cr, Fe) may be typical for Douros synthetic rubies. Most of the EDXRF spectra also indicated the presence of lead, which both

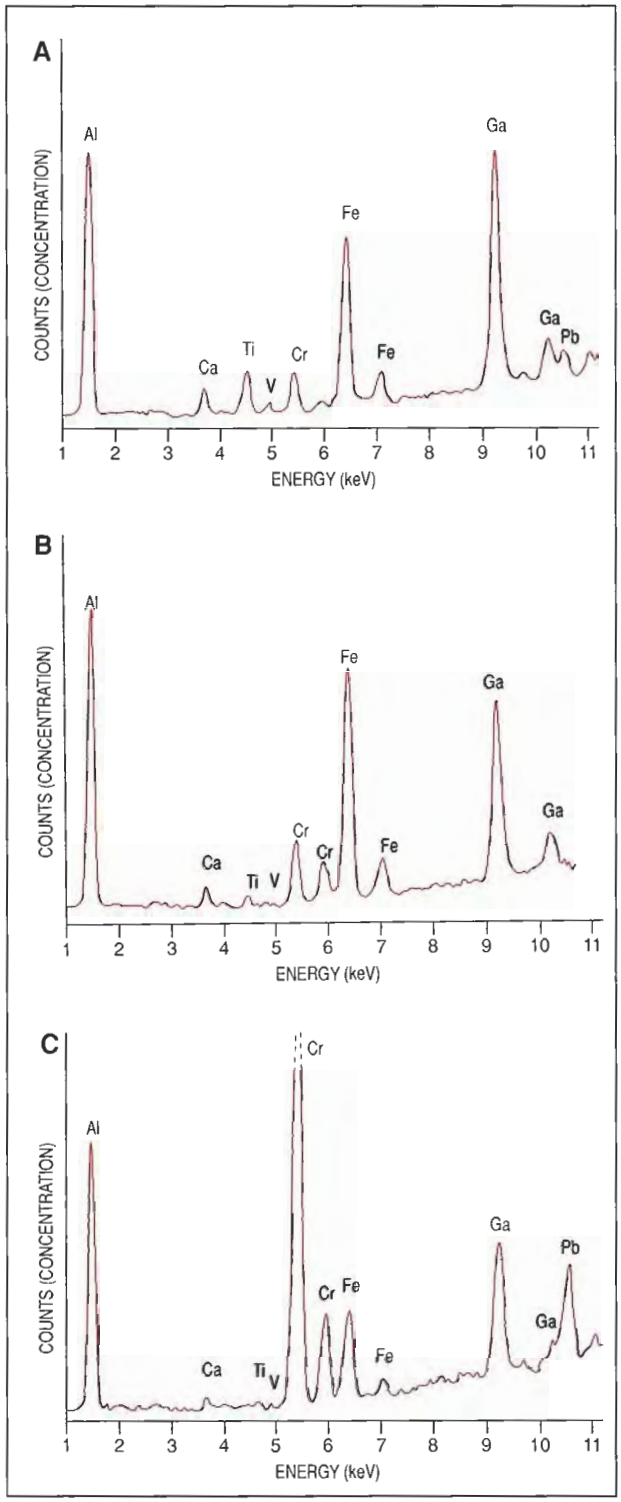

Figure 22. The variability in trace elements in the outermost layers of Douros crystals is evident in these EDXRF spectra of three samples: (A) a tabular crystal with Fe > Cr measured on the c *face; (B) a rhombohedral crystal with Fe > Cr measured on the* r *face; and (C) a rhombohedral crystal with Fe < Cr measured on the* c *face. This last spectrum is also typical for faceted samples.*

SEM-EDS and X-ray diffraction analyses (see below) showed to be a component of the flux used in the growth process. Even in those cases where flux inclusions cannot be seen with high magnification, EDXRF analysis sometimes reveals the presence of Pb peaks as evidence of submicroscopic particles of flux.

EDXRF analysis did not reveal traces of either platinum or iridium (from the crucible) or of lanthanum or bismuth. The latter are typical components of the flux used to grow Ramaura synthetic rubies (Schmetzer, 1986a; Schmetzer et al., 1994).

The quantitative data provided by the microprobe analyses (see Dunn, 1977) revealed only a limited chemical variation within each of five of the six rhombohedral rubies analyzed (three crystals and three faceted samples; table 3). The faceted samples (A, B, and C), as well as the intergrown crystals (D1 and D2), showed distinctly more chromium than iron. In contrast, iron was found to surpass chromium (present in very small amounts) on the rhombohedral face *r* of rough sample E, which was a typical "ruby" red color and had an ordinary chromium absorption spectrum. This indicates a selective compositional zoning with respect to different crystal faces, as well as between late-stage growth layers and the cores, in the rhombohedral crystals. It is consistent with the color zoning observed in the crystals.

Sample D1 showed a distinct zoning with respect to chromium, in the form of a compositional discontinuity between the two parts of the crystal. We recorded Cr_2O_3 values between 0.65 and 0.55 wt.% in the main part, and only 0.18 to 0.10 wt.% in the narrow outermost layer. There was no comparable zoning for iron. This zoning of chromium is consistent with the observation of dark red cores and lighter red or nearly colorless rims in the rhombohedral crystals (figure 11). Since the surface layers are typically thin, they are usually removed during cutting.

The results of microprobe analysis of the slice cut from a tabular crystal are given in table 4. The central part of the crystal (again, see figure 14) consists of two areas of different chromium content. In both areas, which are designated "upper core" and "lower core" in figure 14 and table 4, iron content is low. However, we found no distinct pattern to the distribution of iron and chromium within either core. In contrast, we measured a high variation in chromium and iron contents in the upper and lower surface layers: In both, chromium progressively decreased—and iron progressively increased--from the core side to the surface side. A substitutional exchange of Cr by Fe in these growth zones is evident. We could not detect a systematic variation of titanium in the same scans. We also found that the chromium content decreases from the center (scan A) to the outer zone (scan C) of the crystal (table 4). The data obtained from scan B are intermediate between those of scans A and C.

Scanning Electron Microscopy and X-Ray Diffraction Analysis. SEM-EDS analysis of the residual yellow flux exposed at the surface of some faceted samples showed characteristic X-ray fluo-

TABLE 3. Electron microprobe analyses of five Douros synthetic rubies.[a]

	A	B	C	D			E
Oxide	Faceted (4.21 ct)	Faceted (1.31 ct)	Faceted (1.18 ct)	Intergrowth of two rhombohedral crystals (3.48 ct)			Rhombohedral crystal (7.57 ct) *r* face
				Crystal D1		Crystal D2	
				Core	Surface layer	Core	
Al_2O_3	97.23–98.04	98.12–98.63	97.56–98.29	98.12–98.42	98.68–98.08	97.83–98.64	97.95–100.29
TiO_2	0.00– 0.03	0.01– 0.05	0.00– 0.03	0.00– 0.02	0.00– 0.02	0.00– 0.02	0.01– 0.07
Cr_2O_3	0.79– 0.96	0.60– 0.70	0.77– 0.99	0.55– 0.65	0.10– 0.18	0.47– 0.75	0.01– 0.04
Fe_2O_3	0.03– 0.07	0.04– 0.09	0.09– 0.16	0.03– 0.07	0.05– 0.08	0.03– 0.08	0.13– 0.34
MnO	0.00– 0.02	0.00– 0.02	0.00– 0.01	0.00– 0.02	0.00– 0.01	0.00– 0.02	0.00– 0.01

[a] *Oxides in wt.%; ranges of 30 point analyses performed on each sample. Vanadium was below the detection limit; gallium was not measured.*

rescence lines for lead (figure 23). A silvery metal grain on the surface of one crystal (again, see figure 5) proved to be platinum, probably from the crucible.

An X-ray powder diffraction pattern was prepared from some of the yellow material removed from the surface of one of the crystals (see, e.g., figure 6). The pattern revealed that the material was lead nitrate, $PbNO_3$, which undoubtedly formed from the lead-bearing flux on the surface of the crystal when it was separated from the flux in nitric acid, HNO_3.

DISCUSSION

The present investigation indicates that the new Douros synthetic rubies occur in essentially two types of crystals—(1) rhombohedral and (2) tabular—which differ in habit, structural properties, and compositional characteristics. These two types probably result from the different temperature conditions that occur during the slow cooling that is part of the crystallization process from a flux. The ideal early growth conditions favor the formation of a rhombohedral crystal habit with *c* and *r* faces. When supersaturation decreases, and when the temperature starts to drop, new physical and chemical conditions favor the formation of *d* faces; the development of tabular crystals seems to reflect these later formation conditions. Also, at the end of the growth period, there is less of the dominant color-causing element chromium and more iron, which leads to the formation of near-colorless surface layers.

EDXRF results support this scenario. Spectra taken on the basal plane of tabular Douros synthetic ruby crystals show small chromium peaks and high iron peaks. This agrees with the microprobe analyses taken on a cross-section, as shown in table 4. The complex chemical zoning observed across the tabular crystal is also responsible for the fact that no distinct reading could be taken on this plane with the refractometer. The low-chromium/high-iron content near the surfaces of tabular crystal faces not only explains the near-colorless to light red zones seen along the outermost layers, but also explains the lower intensity or even absence of U.V. fluorescence in these areas.

The EDXRF spectra of rhombohedral crystals revealed a difference in outer-layer composition between the intense red basal faces (Cr > Fe) and the almost-colorless to light red rhombohedral faces (Fe > Cr). Microprobe analyses of the outer layers of two rhombohedral samples (sample E and the surface layer of sample D1, in table 3) also revealed dis-

TABLE 4. Chemical zoning in a tabular crystal of Douros synthetic ruby.[a]

Oxide	Upper layer, confined to *c*	Upper core, confined to *r*	Lower core, confined to *d*	Lower layer, confined to *-c*
Scan A	12 point analyses	17 point analyses	8 point analyses	13 point analyses
Al_2O_3	100.21–99.72	98.66–99.55	98.36–99.73	98.55–99.93
TiO_2	0.00– 0.02	0.00– 0.02	0.00– 0.02	0.00– 0.02
Cr_2O_3	0.04– 1.22[b] surface —> core	1.00– 1.12	1.15– 1.43	1.07– 0.05[b] core <— surface
Fe_2O_3	0.31– 0.11[c] surface <— core	0.09– 0.15	0.08– 0.14	0.15– 0.32[c] core —> surface
MnO	0.00– 0.01	0.00– 0.02	0.00– 0.02	0.00– 0.02
Scan C	7 point analyses	23 point analyses	12 point analyses	8 point analyses
Al_2O_3	98.10–99.35	98.63–99.75	98.42–99.35	98.67–99.52
TiO_2	0.00– 0.02	0.00– 0.02	0.00– 0.01	0.00– 0.02
Cr_2O_3	0.04– 0.90[b] surface —> core	0.67– 0.81	0.92– 1.03	0.88– 0.02[b] core <— surface
Fe_2O_3	0.23– 0.11[c] surface <— core	0.13– 0.15	0.11– 0.15	0.10– 0.27[c] core —> surface
MnO	0.00– 0.01	0.00– 0.02	0.00– 0.02	0.00– 0.01

[a]*Oxides in wt.%; ranges of electron microprobe analyses; scans along the c-axis between the upper and lower basal pinacoids; thickness of the tabular crystal is 2.2 mm (see text for further details of sample preparation). Vanadium was below detection limit; gallium was not measured.*
[b]*Continuous decrease in chromium from core to surface layer in c face areas.*
[c]*Continuous increase in iron from core to surface layer in c face areas.*

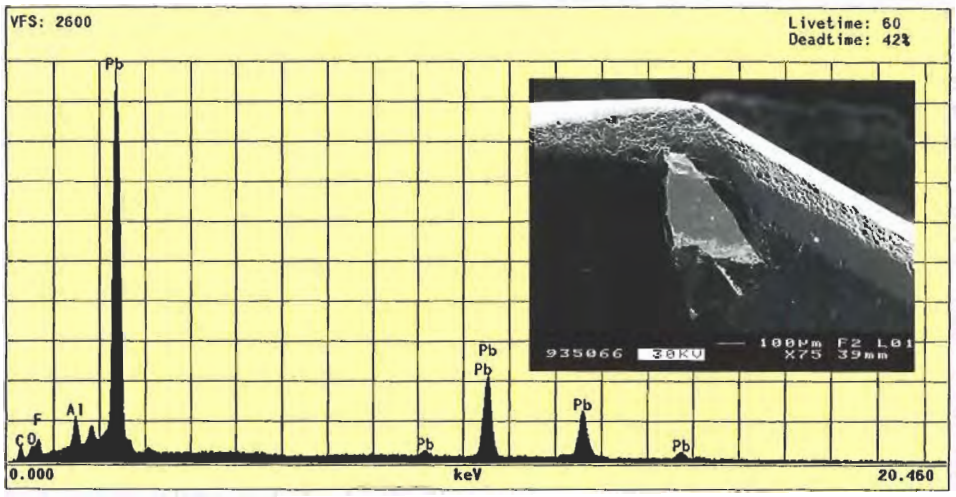

Figure 23. This scanning electron micrograph shows the corner of a faceted ruby with a yellow material that was analyzed by SEM-EDS. The resulting spectrum indicates that lead (Pb) is the main component in this flux particle.

tinctly lower chromium and higher iron concentrations in these regions, as compared to sample D2 and analyses of the faceted samples. (Note that only the core area of D2 was analyzed, because the specimen had been cut such that there was no distinct outer layer on the new surface.)

Because EDXRF analyses were performed on the table facets of the faceted rubies, and there is no general rule for the crystallographic orientation of the tables, we also examined random orientations and cutting angles of the crystals. We found that the cut Douros synthetic rubies usually exhibited the same chemical characteristics as the cores (i.e., from which the colorless outer layers were removed) of rhombohedral material. This is consistent with our microscopic observations. Microprobe analyses of three faceted samples (A, B, and C of table 3), as compared to analyses of the core of rhombohedral crystal D1 and crystal D2, confirmed the high chromium and low iron concentrations.

With careful microscopic examination, we saw color zoning in all of the rhombohedral Douros crystals in the form of thin colorless outer layers on the *d* and *r* faces. R.I. differences between the *r* and *c* faces (table 1) and the different reactions to ultraviolet radiation of these external layers agree with the results of X-ray fluorescence and microprobe investigations. The zones with less-intense U.V. fluorescence were also mentioned by Smith and Bosshart (1993) for rhombohedral crystals.

SEPARATION OF DOUROS SYNTHETIC RUBY FROM NATURAL RUBY

Faceted Douros synthetic rubies may show a number of characteristic features that distinguish them from natural rubies if they are inspected carefully. Although yellow flux inclusions (e.g., figure 16) are probably the easiest means of identification, such large flux inclusions were relatively rare in the faceted stones we examined. Because the flux consists of a lead compound, however, Pb may be identified by EDXRF as a trace element in the bulk composition. Lead is not found in natural rubies (except possibly in fissures or cavities, if a stone was polished on a lead wheel), and few natural rubies contain inclusions that resemble the typical large flux inclusions.

Structural characteristics—such as the umbrella-shaped internal *d* growth zones (figure 15) or the near-colorless surface layers (figure 7)—cannot be expected in each sample. These properties are confined to the intermediate and outer growth areas, which would probably be at least partly removed by the bruting or cutting process. The characteristic twinning observed in tabular crystals is not present in cut stones from rhombohedral rough.

As demonstrated above, trace-element ratios may vary within a sample, depending on the orientation of the crystal measured. We usually found distinct amounts of Ti, Fe, and Ga, in addition to Cr, but V, if present, was below the detection limit of EDXRF.

Natural rubies usually have crystal faces different from those observed in the Douros synthetic ruby. They often show intercalated fine twin lamellae in one, two, or three spatial directions, with characteristic intersection lines. We did not see such structural features in the Douros material. Most Douros synthetic crystals did reveal growth planes confined to color zoning that do not occur in natural material in this form.

Even after heat treatment, mineral inclusions in ruby may exhibit crystal shapes that will help characterize the host stone as natural. Rutile needles, or the traces that remain after heat treatment, were not present in the Douros synthetic rubies we

examined. However, "veils" or fissures such as those shown in figure 20 could very well be confused with similar-appearing features that are commonly seen in natural ruby.

CONCLUSION

The Douros flux-grown synthetic ruby has been in the marketplace since January 1993. The manufacturers, John and Angelos Douros, report that they have been producing approximately 2,000 ct per month. The Douros product most closely resembles the Ramaura flux-grown synthetic ruby, with characteristics that are not seen in synthetic rubies by other manufacturers.

Most of the gemological properties of the Douros material overlap those of natural rubies. It is most easily identified as a synthetic when there are large inclusions of flux, which are readily recognized by their coarseness, yellow color, crazed appearance, and bubbles. If no characteristic flux inclusions are seen, a combination of chemical analysis (to reveal the presence of Pb and compare the contents of V, Ti, Cr, Fe, and Ga with those typically encountered in natural rubies) and immersion microscopy (to reveal characteristic crystal-growth patterns and color zoning) should provide the evidence to distinguish this new synthetic ruby from its natural counterpart.

Acknowledgments: The authors are grateful to Prof. R. Guggenheim and Mr. D. Mathys, of the Laboratory for Scanning Electron Microscopy of Basel University, for their help in analyzing the flux. Dr. O. Medenbach, of the Institute for Mineralogy of Bochum University, helped with crystal drawings and X-ray diffraction analysis. Except where noted, all of the photomicrographs are by the authors.

REFERENCES

Bosshart G. (1982) Distinction of natural and synthetic rubies by ultraviolet spectrophotometry. *Journal of Gemmology*, Vol. 8, pp. 145–160.

Bosshart G. (1983) Ramaura—eine neue Rubinsynthese (erste Untersuchungsergebnisse). *Zeitschrift der Deutschen Gemmologischen Gesellschaft*, Vol. 32, pp. 164–171.

Burch C.R. (1984) Some observations on a Kashan synthetic ruby. *Journal of Gemmology*, Vol. 19, pp. 54–61.

Douros J., Douros A. (1993) Cultivated ruby from Greek production. *Chrysotechni*, Vol. 4, No. 45, p. 56.

Dunn P. (1977) The use of the electron microprobe in gemology. *Journal of Gemmology*, Vol. 15, No. 5, pp. 248–258.

Hänni H.A., Bosshart G. (1993) Flux synthetic ruby alleged European production. *ICA Early Warning Flash*, Laboratory Alert No. 71, June 8, 1993.

Hänni H.A., Schmetzer K. (1993) First results on a new flux-grown synthetic ruby (Douros) produced in Greece. In *Abstracts of the 24th International Gemological Conference, Paris, France, 2–15 October 1993*, Association Française de Gemmologie, Paris, 1993.

Kane R.E. (1983) The Ramaura synthetic ruby. *Gems & Gemology*, Vol. 19, No. 3, pp. 130–148.

Kiefert L., Schmetzer K. (1991) The microscopic determination of structural properties for the characterization of optical uniaxial natural and synthetic gemstones. Part 1: General considerations and description of the method. *Journal of Gemmology*, Vol. 22, pp. 344–354.

Muhlmeister S., Devouard B. (1991) Determining the natural or synthetic origin of rubies using energy-dispersive X-ray fluorescence (EDXRF). In A. S. Keller, Ed., *Proceedings of the International Gemological Symposium 1991*, Gemological Institute of America, Santa Monica, CA, pp. 139–140.

Schmetzer K. (1986a) *Natürliche und synthetische Rubine—Eigenschaften und Bestimmung*. Schweizerbart, Stuttgart.

Schmetzer K. (1986b) An improved sample holder and its use in the distinction of natural and synthetic ruby as well as natural and synthetic amethyst. *Journal of Gemmology*, Vol. 20, pp. 20–33.

Schmetzer K. (1987) On twinning in natural and synthetic flux-grown ruby. *Journal of Gemmology*, Vol. 20, pp. 294-305.

Schmetzer K., Bank H. (1981): The color of natural corundum. *Neues Jahrbuch für Mineralogie Monatshefte*, Vol. 1981, pp. 59–68.

Schmetzer K., Smith C.P., Bosshart G., Medenbach O. (1994) Twinning in Ramaura synthetic rubies. *Journal of Gemmology*, Vol. 24, pp. 87–93.

Smith C.P., Bosshart G. (1993) New flux-grown synthetic rubies from Greece. *JewelSiam*, Vol. 4, No. 4, pp. 106–114; No. 5, p. 16.

Stern W.B., Hänni H.A. (1982) Energy dispersive X-ray spectrometry: A non-destructive tool in gemology. *Journal of Gemmology*, Vol. 18, pp. 285–296.